Observation of the large magnetocaloric effect in an orbital–spin-coupled system MnV_2O_4

2009 J. Phys.: Condens. Matter 21 436010

(http://iopscience.iop.org/0953-8984/21/43/436010)

J. Phys.: Condens. Matter **21** (2009) 436010 (5pp) doi:10.1088/0953-8984/21/43/436010

Observation of the large magnetocaloric effect in an orbital–spin-coupled system MnV_2O_4

X Luo[1], Y P Sun[1,2,3], L Hu[1], B S Wang[1], W J Lu[1], X B Zhu[1], Z R Yang[1] and W H Song[1]

[1] Key Laboratory of Materials Physics, Institute of Solid State Physics, Chinese Academy of Sciences, Hefei 230031, People's Republic of China
[2] High Magnetic Field Laboratory, Chinese Academy of Sciences, Hefei 230031, People's Republic of China

E-mail: ypsun@issp.ac.cn

Received 18 August 2009, in final form 18 September 2009
Published 8 October 2009
Online at stacks.iop.org/JPhysCM/21/436010

Abstract
The magnetocaloric effect (MCE) in an orbital–spin-coupled spinel vanadate MnV_2O_4 is investigated by magnetization measurement. MnV_2O_4 has ferrimagnetic ordering occurring at $T_C = 57$ K. The maximum magnetic entropy change reaches 14.8 and 24.0 J kg^{-1} K^{-1} for field changes of 0–2 and 0–4 T, respectively. The maximum adiabatic temperature is about 2.9 K for a magnetic field change of 2 T. Except for the spin entropy change, the observed giant MCE is suggested to be related to the orbital entropy change due to the change of the orbital state of V^{3+} induced by an applied magnetic field around T_C.

(Some figures in this article are in colour only in the electronic version)

1. Introduction

Magnetic materials with a large magnetocaloric effect (MCE) at temperatures below 70 K have attracted much research interest due to their potential environmental advantages over gas liquefiers [1, 2]. The key problem in application of magnetic refrigeration is to seek those materials that are cheaper but display a larger MCE. Mostly, rare-earth materials and their alloys show excellent magnetocaloric properties because of their large magnetic moment [1–6]. However, rare-earth metals are in general expensive, and therefore there is a strong incentive to search for new inexpensive materials that exhibit a large MCE below 70 K.

Recently, the spinel vanadium oxide, with formula AV_2O_4, has been extensively studied due to its interesting physical properties [7–19]. In this series of compounds, there is antiferromagnetic (AFM) (ZnV_2O_4, MgV_2O_4, CdV_2O_4 etc) or ferrimagnetic (MnV_2O_4) ordering, which are dominated by direct t_{2g}–t_{2g} interaction between neighboring V^{3+} spins ($S = 1$) or by the superexchange (SE) interaction through the oxygen 2p orbital between V^{3+} and Mn^{2+} ($S = 5/2$) spins [15]. A structure phase transition into a tetragonal phase is presumably induced by the ordering of V orbitals below the magnetic ordering temperature. Katsufuji and co-workers [13, 15] reported a magnetic field 'switching' of the crystal structure in MnV_2O_4. It was demonstrated that the applied magnetic field enhances the evolution of a ferromagnetic (FM) moment on the V site and induces an orbital ordering (OO) and the structural phase transition into a tetragonal phase. In other words, the applied magnetic field can easily change the lattice structure and the spin configuration in MnV_2O_4. In general, the MCE is expected to be high across a magnetic phase transition or structural phase transition, and this gives us the motivation to study the MCE of MnV_2O_4 around T_C. In this paper, the MCE of MnV_2O_4 is investigated by dc magnetic measurements, indicating that MnV_2O_4 is probably a promising candidate as a working material below 70 K in magnetic refrigeration technology.

2. Experimental details

Polycrystalline samples of MnV_2O_4 were prepared by the standard solid-state synthesis method. A stoichiometric

[3] Author to whom any correspondence should be addressed.

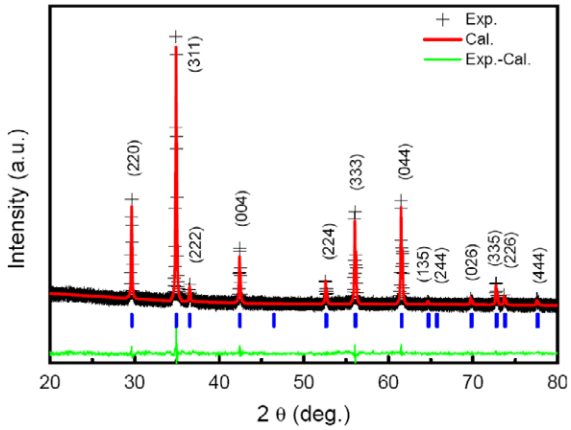

Figure 1. X-ray powder diffraction pattern (plus marks) and Rietveld refinement pattern (solid line) of MnV_2O_4 at room temperature. The vertical marks indicate the position of Bragg peaks, and the solid line at the bottom corresponds to the difference between observed and calculated intensities.

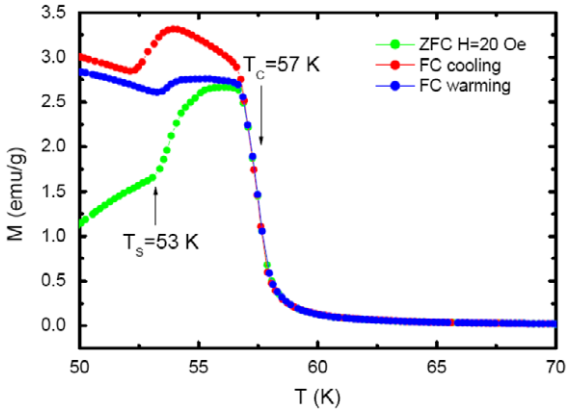

Figure 2. Temperature dependence of magnetization recorded in the ZFC, FCC and FCW modes under an applied magnetic field $H = 0.002$ T. T_C and T_S correspond to the ferrimagnetic ordering temperature and the low temperature structural phase transition, respectively.

mixture of MnO and V_2O_3 was carefully crushed and pressed in the form of bars. These bars were placed in a Pt crucible which was sealed in an evacuated quartz tube ($\sim 10^{-5}$ Torr). The tube was heated at 950 °C for 40 h. The phase purity of the sample was examined by powder x-ray diffraction (XRD) using Cu Kα radiation at room temperature. The magnetization measurement was performed with a Quantum Design (QD) superconducting quantum interference device (SQUID) system ($1.9\ \text{K} \leqslant T \leqslant 400\ \text{K}$, $0\ \text{T} \leqslant H \leqslant 5\ \text{T}$).

3. Results and discussion

Figure 1 displays the experimental XRD and the Rietveld analysis patterns of MnV_2O_4 with 2θ scanning from 20° to 80° at room temperature. All diffraction peaks can be indexed into a face-centered cubic cell ($Fd\bar{3}m$) with the lattice parameter $a = 8.5227$ Å obtained from the Rietveld analysis. The lattice parameter is consistent with reported data [12, 15, 16].

Figure 2 shows the temperature dependence of magnetization (M–T) in an applied magnetic field $H = 0.002$ T under zero-field cooling (ZFC), field-cooling cooling (FCC) and field-cooling warming (FCW) modes. It indicates that ferrimagnetic ordering occurs at $T_C = 57$ K, defined as the temperature of the maximum slope in the M–T curves. Below T_C there is a difference in the ZFC and FC data, which is due to a spin-glass-like ground state developing at low temperatures [21]. Both FCC and FCW curves show no hysteresis, which demonstrates the second-order character of the magnetic transition. The second transition taking place at lower temperature ($T_S = 53$ K) corresponds to a falling of M with temperature decreasing in the FCW mode, which might be related to the structural phase transition induced by the antiferro-type ordering of the V t_{2g} orbitals. A clear hysteresis is a typical characteristic of the first-order transition. The magnetic measurement is in agreement with the previously reported results [15, 17].

In order to obtain the change in magnetic entropy, isothermal magnetization curves are recorded in the temperature range of 20–90 K in a magnetic field up to 4.5 T. The measurement results are shown in figure 3(a), where the blue lines show the magnetization curves around T_C. The inset of figure 3(a) shows the field dependence of the reversible magnetization around T_C; the bubble-like hysteresis is related to the field-induced structural phase transition [17]. The magnetic entropy change is given by

$$\Delta S_m(T, H) = S_m(T, H) - S_m(T, 0) = \int_0^H \left(\frac{\partial M}{\partial T}\right)_H \mathrm{d}H, \tag{1}$$

and can be evaluated by the expression

$$|\Delta S_m| = \sum_i \frac{M_i - M_{i+1}}{T_{i+1} - T_i} \Delta H_i, \tag{2}$$

where M_i is the magnetization at temperature T_i.

Magnetic entropy change versus temperature curves derived from equation (2) are shown in figure 3(b). In the vicinity of T_C, the maximum entropy change $|\Delta S_m^{max}|$ is 14.8 and 24.0 J kg^{-1} K^{-1} for fields of 2 and 4 T, respectively. According to mean field theory, the relation between magnetic entropy and magnetic field near the magnetic phase transition is described as [20]

$$\Delta S_m \cong -1.07 q R \left(\frac{g \mu_B J H}{k T_C}\right)^{2/3} \tag{3}$$

where q is the number of magnetic ions, R is the gas constant and g is the Landé factor. The inset of figure 3(b) shows the $H^{2/3}$ dependence of ΔS_m for MnV_2O_4. It is found that ΔS_m has a good linear dependence on $H^{2/3}$ at low fields, implying a second-order character for the magnetic transition. However, the field $H^{2/3}$ dependence of magnetic entropy deviates upward from linearity above 2 T, which is related to the magnetic-field-induced structural phase transition [13, 15]. The increased magnetic entropy might originate from the orbital change of V^{3+} ions, which is caused by the presence of the antiferro-type orderings of the V t_{2g} orbitals above 2 T. The

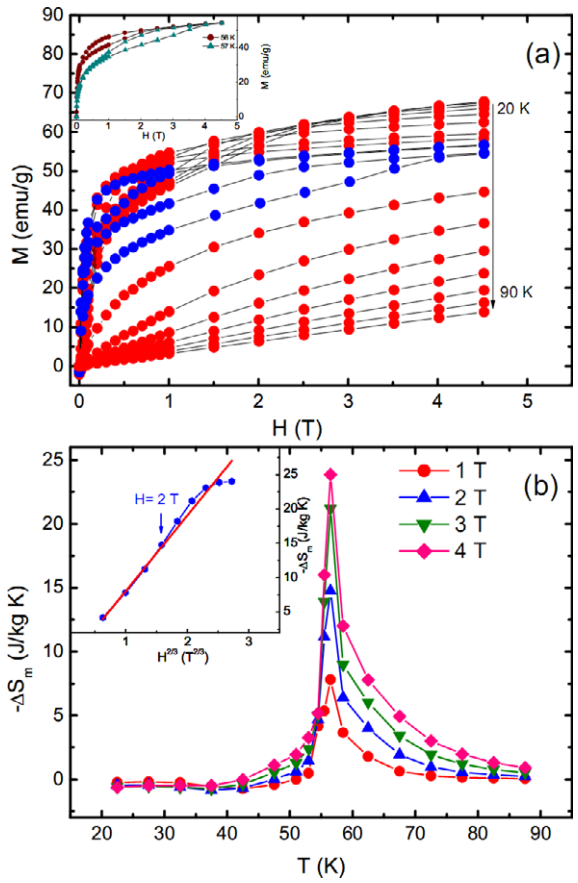

Figure 3. (a) Magnetization as a function of applied field for MnV_2O_4 between 20 and 90 K. The blue circle dots and lines correspond to temperatures around T_C. The inset shows the field dependence of reversible magnetization around T_C. (b) Entropy changes in MnV_2O_4 extracted from magnetization measurements with magnetic field changes from 0 to 1, 2, 3 and 4 T. The inset shows the relation between maximum ΔS and $H^{2/3}$ near the magnetic transition temperature. The straight line gives a linear fit to data.

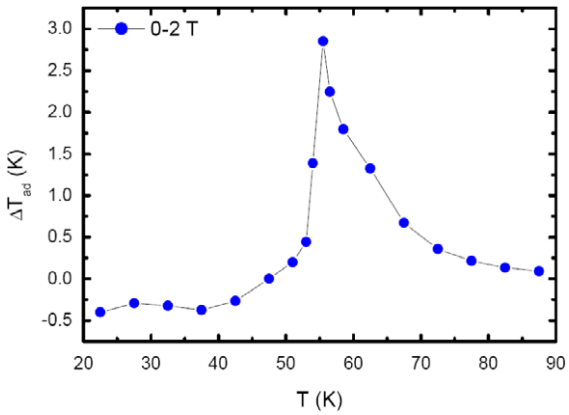

Figure 4. Temperature dependence of the adiabatic temperature change ΔT_{ad} in MnV_2O_4 induced by a magnetic field change of 0–2 T.

reason why the values of magnetic entropy tend to saturation at high fields is not yet clear, and further investigation is needed in the future. However, the large magnetic entropy change ($-\Delta S_m$) indicates that MnV_2O_4 belongs to a class of giant MCE materials. The giant MCE related to the field-induced magnetic transition obtained in MnV_2O_4 is compared with that observed in Ho_5Pb_2 [22], DySb [28] and $ErRu_2Si_2$ [26] compounds in which a field-induced AFM to FM transition occurs. Table 1 shows the magnetocaloric parameters of some respective giant MCE materials working at low temperatures. It demonstrates that the observed value of $-\Delta S_M$ for MnV_2O_4 is quite large in comparison with that of some giant MCE materials, especially at low fields ($H = 2$ T).

It is well known that another important parameter for a MCE material is the adiabatic temperature change ΔT_{ad}. Based on thermodynamics, the adiabatic temperature change at an arbitrary temperature T_0 can be expressed as

$$\Delta T \cong -\Delta S_m(T_0, H)\frac{T_0}{C_p(T_0, H)} \qquad (4)$$

where C_p is the specific heat. The data for heat capacity in a field of $H = 2$ T were obtained from the [17]. Figure 4 shows the temperature dependence of the adiabatic temperature change ΔT_{ad} for the applied magnetic field $H = 2$ T. The peak value of ΔT_{ad} is about 2.9 K for a magnetic field variation of 0–2 T. The relative cooling power (RCP), evaluated by RCP $= -\Delta S_M^{max} \times \delta T$, is about 46.7 and 86.1 J kg^{-1} for 2 T and 4 T, respectively. The transition temperature (T_M), together with the maximum values of magnetocaloric parameters ($-\Delta S_M$ and ΔT_{ad}) and relative cooling power (RCP) under 2 and 4 T for MnV_2O_4 and various giant MCE materials are listed in table 1 for comparison. This table shows that both ΔT_{ad} and RCP values are comparable with those of some giant MCE materials and the maximum value of $-\Delta S_M$ is larger than that of the potential promising magnetic refrigerant materials at 2 and 4 T at low temperatures. Therefore, the large magnetic entropy and adiabatic temperature change imply that the spinel vanadium MnV_2O_4 is probably a promising candidate working material below 70 K in magnetic refrigeration technology. In addition, there are also some other advantages of MnV_2O_4 as a magnetic refrigerant material: (1) the reversible MCE in low fields (<2 T); (2) the relatively low cost of components and fabrication using MnO powder and V_2O_3.

As is well known, a large MCE is usually related to two factors: the large saturation magnetization (M_S) and the rapid change of magnetization around the magnetic phase transition. From the isothermal magnetization curve at 20 K, the M_S value is about 65 emu g^{-1} (2.6 μ_B/f.u.). The change of magnetization is not very sharp around T_C (the temperature interval between the PM and FM state is about 2 K obtained from figure 2). The above two values are not comparable with those of conventional MCE materials [22–28]. For MnV_2O_4, these two factors do not seem to play the key role in the MCE. There might exist a special character in our studied system. We turn to the magnetic structure of the orbital–spin-coupled system MnV_2O_4. In general, the evolution of MnV_2O_4's magnetism might be described as follows: the collinear ferrimagnetic ordering (T_C), where the Mn spins and the V spins are aligned in opposite direction and the FM coupling is within the V^{3+} sublattice, occurs at about

Table 1. The transition temperature (T_M), the maximum values of magnetocaloric parameters ($-\Delta S_M$ and ΔT_{ad} as well as RCP) under 2 and 4 T for MnV_2O_4 and various giant MCE materials.

Material	T_M (K)	$-\Delta S_M$ (J kg^{-1} K^{-1})/(mJ cm^{-3} K^{-1}) 2 T	4 T	RCP (J kg^{-1}) 2 T	4 T	ΔT_{ad} (K) 2 T	Reference
MnV_2O_4	57	14.8 (70.2)	24.0 (113.8)	46.7	86.1	2.9	Present work
Ho_5Pd_2	25	~7	~15	~204	~578	—	[21]
$CdCr_2S_4$	87	3.92 (16.7)	7.04 (30.0)	~130	~360	2.6	[22]
MnSi	~40	2.2 (13.0)	3.22 (19.0)	21.39	47.42	2.6	[23]
$Dy_{50}Gd_7Al_{23}Co_{20}$	26	4.33	—	173	—	—	[24]
$ErRu_2Si_2$	5.5	~11 (97.4)	~15 (132.8)	~55	—	5.9	[25]
$Eu_8Ga_{16}Ge_{30}$	13	~8.5	—	87	—	—	[26]
DySb	11	—	~12 (97.3)	~34	—	—	[27]

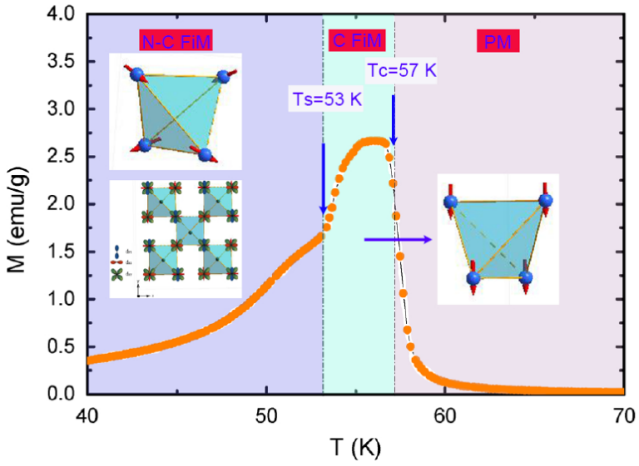

Figure 5. Schematic representations of the evolution of MnV_2O_4s magnetism and the magnetization dependence of temperature under $H = 0.002$ T in the ZFC mode. The Mn moments are aligned upwards (not shown in the figure). N–C FiM, C FiM and PM denote the non-collinear ferrimagnetic, collinear ferromagnetic and paramagnetic phases, respectively.

57 K. With decreasing temperature, through the SE interaction between the V^{3+} ions, where the FM spin order favors an AFM orbital coupling within the t_{2g} orbitals of V^{3+} ions, and with the help of the Jahn–Teller effect induced by the VO_6 octahedron, an OO with tetragonal distortion occurs at T_S (one t_{2g} electron of V^{3+} occupies the d_{xy} orbital and another t_{2g} electron locates the d_{yz} and d_{zx} orbitals alternately along the c axis). The tetragonal structural distortion stabilizes a canting within the V spins, leading to triangular ferrimagnetic order (non-collinear ferrimagnetic order). Simple schematic representations are shown in figure 5. The maximum of the magnetic entropy obtained from the experiment is around T_C, which is higher than T_S. The magnetic hysteresis occurs in the field dependence of magnetization above T_S, as shown in the inset of figure 3(a), which is related to the OO of V ions. In other words, though the temperature of the maximum of the magnetic entropy is higher than T_S, the OO of V^{3+} can also been induced by applied magnetic fields due to the strong coupling between the spin, orbital and lattice degrees of freedom in MnV_2O_4 [15]. Because one electron of the V ion occupies the superposition of the yz and zx orbitals, the angular momentum is not totally quenched for the V orbitals, i.e. total angular momentum $\boldsymbol{J}' = \boldsymbol{L}' + \boldsymbol{S}$, the change of orbital order/disorder can be reflected in the isothermal magnetization. The calculated magnetic entropy is not only the spin entropy coming from the ferrimagnetic to PM transition but also the orbital entropy induced by the OO of V^{3+}. Thus, the large MCE of MnV_2O_4 is different from the conventional giant MCE materials where the giant MCE effect is mainly from the contribution of spin order–disorder. The entropy change of MnV_2O_4 is derived from the spin entropy and orbital entropy around T_C. The contribution of orbital entropy might be an important part of the magnetic entropy of MnV_2O_4. The similar large MCE is also observed near the charge/orbital ordering transition in manganites [2, 29, 30]. The strong coupling between orbital and spin degrees of freedom in the t_{2g} states at the V site is mainly responsible for the OO induced by the magnetic field about T_S in the orbital–spin-coupled system studied here. The large MCE suggests that the spinel vanadate MnV_2O_4 is probably a promising candidate as a working material below 70 K in magnetic refrigeration technology. However, more detailed study is needed in vanadates as the origin of large magnetic entropy change deserves to be investigated further.

4. Conclusion

In summary, MnV_2O_4 shows a large magnetic entropy change near $T_C = 57$ K. A magnetic field induces a structural phase transition, leading to large magnetic entropy changes ~14.8 and 24.0 J kg^{-1} K^{-1} for field changes of 0–2 and 0–4 T. The maximum ΔT_{ad} is about 2.9 K for a magnetic field change of 2 T. Except for the spin entropy change, the observed giant MCE is suggested to be related to the orbital entropy change due to the change of the orbital state of V^{3+} ions with an applied field around T_C. The study of MnV_2O_4 may give some indications for exploring spinel vanadates for magnetic refrigeration technology.

Acknowledgments

This work was supported by the National Key Basic Research under contract no. 2007CB925002, the National Science Foundation of China under contract nos 10974205, 10774146, 10774147, 50672099, 10804111 and the Director's Fund of Hefei Institutes of Physical Science, Chinese Academy of Sciences.

References

[1] Tishin A M and Spichkin Y I 2003 *The Magnetocaloric Effect and its Applications* (London: Institute of Physics)
[2] Gschneidner K A Jr, Pecharsky V K and Tsokol A O 2005 *Rep. Prog. Phys.* **68** 1479 and references herein
[3] Pecharsky V K and Gschneidner K A Jr 1997 *Phys. Rev. Lett.* **78** 4494
[4] Wada H and Tanabe Y 2001 *Appl. Phys. Lett.* **79** 3302
[5] de Oliveira I G, von Ranke P J, El Massalami M and Chaves C M 2005 *Phys. Rev.* B **72** 174420
[6] Singh N K, Agarwal S, Suresh K G, Nirmala R, Nigam A K and Malik S K 2005 *Phys. Rev.* B **72** 014452
[7] Mamiya H, Onoda M, Furubayashi T, Tang J and Nakatani I 1997 *J. Appl. Phys.* **81** 5289
[8] Ueda Y, Fujiwara N and Yasuoka H 1997 *J. Phys. Soc. Japan* **66** 778
[9] Nishiguchi N and Onoda M 2002 *J. Phys.: Condens. Matter* **14** L551
[10] Tsunetsugu H and Motome Y 2003 *Phys. Rev.* B **68** 060405(R)
Motome Y and Tsunetsugu H 2005 *Prog. Theor. Phys. Suppl.* **160** 203
Motome Y and Tsunetsugu H 2005 *J. Phys. Soc. Japan* **74** 208
[11] Tchernyshyov O 2004 *Phys. Rev. Lett.* **93** 157206
[12] Plumier R and Sougi M 1987 *Solid State Commun.* **64** 53
Plumier R and Sougi M 1989 *Physica* B **155** 315
[13] Adachi K, Suzuki T, Kato K, Osaka K, Takata M and Katsufuji T 2005 *Phys. Rev. Lett.* **95** 197202
[14] Maitra T and Valentí R 2007 *Phys. Rev. Lett.* **99** 126401
[15] Suzuki T, Katsumura M, Taniguchi K, Arima T and Katsufuji T 2007 *Phys. Rev. Lett.* **98** 127203
[16] Zhou H D, Lu J and Wiebe C R 2007 *Phys. Rev.* B **76** 174403
[17] Hardy V, Bréard Y and Martin C 2008 *Phys. Rev.* B **78** 024406
[18] Garlea V O, Jin R, Mandrus D, Roessli B, Huang Q, Miller M, Schultz A J and Nagler S E 2008 *Phys. Rev. Lett.* **100** 066404
[19] Sarkar S, Maitra T, Valentí R and Saha-Dasgupta T 2009 *Phys. Rev. Lett.* **102** 216405
[20] Oesterreicher H and Parker F T 1984 *J. Appl. Phys.* **55** 4334
[21] Baek S H, Choi K Y, Reyes A P, Kuhns P L, Curro N J, Ramanchandran V, Dalal N S, Zhou H D and Wiebe C R 2008 *J. Phys.: Condens. Matter* **20** 135218
[22] Samanta T, Das I and Banerjee S 2007 *Appl. Phys. Lett.* **91** 082511
[23] Yan L Q, Shen J, Li Y X, Wang F W, Jiang Z W, Hu F X, Sun J R and Shen B G 2007 *Appl. Phys. Lett.* **90** 262502
[24] Arora P, Chattopadhyay M K and Roy S B 2007 *Appl. Phys. Lett.* **91** 062508
[25] Luo Q, Zhao D Q, Pan M X and Wang W H 2007 *Appl. Phys. Lett.* **90** 211903
[26] Samanta T, Das I and Banerjee S 2007 *Appl. Phys. Lett.* **91** 152506
[27] Phan M H, Woods G T, Chaturvedi A, Stefanoski S, Nolas G S and Srikanth H 2008 *Appl. Phys. Lett.* **93** 252505
[28] Hu W J, Du J, Li B, Zhang Q and Zhang Z D 2008 *Appl. Phys. Lett.* **92** 192505
[29] Biswas A, Samanta T, Banerjee S and Das I 2008 *Appl. Phys. Lett.* **92** 212502
[30] Karmakar S, Bose E, Taran S, Chaudhuri B K, Sun C P and Yang H D 2008 *J. Appl. Phys.* **103** 023901